

Coda-Wave Interferometry in Finite Solids: Recovery of *P*-to-*S* Conversion Rates in an Elastodynamic Billiard

Oleg I. Lobkis and Richard L. Weaver

Theoretical and Applied Mechanics, University of Illinois, 104 South Wright Street, Urbana, Illinois 61801, USA

(Received 3 February 2003; published 27 June 2003)

We study the temperature dependence of diffuse reverberant ultrasound in elastic bodies. Transient wave forms are found to undergo an almost pure dilation of 0.0277% per degree, related to the temperature dependence of wave speeds. The wave forms also suffer a distortion that, we argue, depends on the rate of conversion between the dilatational (*P*) and shear (*S*) waves. Distortion is found to scale in a manner consistent with theoretical arguments but also appears to be a function of the degree of ray chaos in the body, indicating that the mixing rates are slower in more regular bodies.

DOI: 10.1103/PhysRevLett.90.254302

PACS numbers: 43.35.+d, 05.45.Mt, 05.60.Gg

Diffuse classical wave fields, whether made diffuse by multiple scatterings or reflections, offer an attractive venue for the exploration of wave statistics in general and mesoscopic issues in particular. Ultrasound and microwaves [1–7] are particularly convenient in that current laboratory technology allows access, not only to intensities and spectra, but also to their fields and to the time domain. In the absence of inelastic scattering a field which is diffuse and thus nominally incoherent nevertheless maintains residual coherence that can lead to striking phenomena. Coherent backscatter [8], Anderson localization [9], random-matrix-like spectral statistics [10], and long range field-field correlations [11] are among these.

Here we explore the effect of temperature changes on the diffuse field (the “coda”) formed by multiply reflected ultrasonic waves in a reverberant three-dimensional elastic body. The work may be considered an extension of ideas advanced elsewhere [12–15], often with an emphasis on the first effect of temperature changes, viz., a wave form dilation due to wave speed decrease. The present work differs in that here we focus on the decay of correlation and demonstrate that this decay is an interesting system-dependent quantity. It is an analog to mesoscopic conductance fluctuations in quantum dots but has a value in its own right as related to mode conversion rates between the *P* and *S* (dilatational and shear) waves which constitute the diffuse elastic wave field, and thus in general to the dynamics of the field’s energy distribution, and, in particular, to the chaos of the ray trajectories.

The laboratory configuration is illustrated in Fig. 1. A transient piezoelectric pulse is applied to a 2 mm diameter pin transducer (useful frequency range 0.1 to 2 MHz in mechanical (light oil) contact with an aluminum alloy block. Specimen sizes ranged from 60 to 3000 cm³. A reed relay, as described elsewhere [8], isolated the response from source circuitry; the resulting acoustic signal was amplified, digitized, and examined as a function of specimen temperature. The specimen was allowed to

cool, from initial temperatures of about 45 °C to 20 °C. Temperature was monitored by a thermocouple, with precision ±0.03 °C. The test was conducted in a vacuum, thus eliminating convective, and most conductive, mechanisms. Typical cooling rates (an exponential relaxation to room temperature) were of order 10⁻⁴/sec. This is consistent with theoretical estimates based on Steffan-Boltzman radiative cooling and the known heat capacity of aluminum. Based on the known thermal conductivity of aluminum, we determine that the specimen temperature was uniform to within better than 0.01 °C.

Figure 2 shows a short window on the signal from different temperatures but the same age, 10 msec, corresponding to a shear wave travel of 30 m, long compared with specimen size. The two signals are almost identical except for a relative displacement of 2.8 μsec.

The change is quantifiable by forming a normalized cross correlation between the signals obtained at different temperatures.

$$X(\varepsilon) = \frac{\int S_{T_1}(t)S_{T_2}(t\{1 + \varepsilon\})dt}{\sqrt{\int S_{T_1}^2(t)dt \int S_{T_2}^2(t\{1 + \varepsilon\})dt}},$$

where the integrals are over a short time window centered

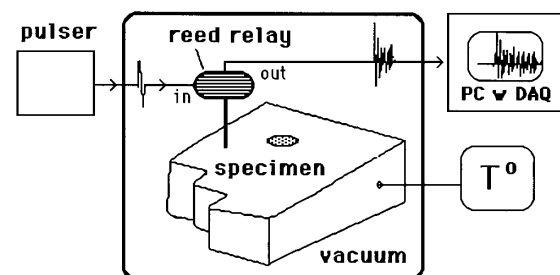


FIG. 1. Laboratory configuration. An aluminum specimen, typically with nonparallel faces and a defocusing cylindrical hole, is allowed to cool in a vacuum as temperature and ultrasonic response are monitored. A reed relay isolates the response from the pulser.

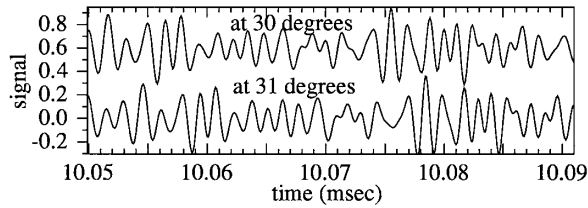


FIG. 2. Signals taken in the same time window are compared for different sample temperatures. An offset has been added to aid visibility.

on an “age” A . If the two signals differ only by a dilation, then X is maximal, and unity, at a value of ε equal to that dilation. Any difference from unity corresponds to a change in signals that cannot be comprehended by a simple dilation. Such a difference is termed a distortion: $D = \ln X_{\max}$. Figure 3 shows a typical plot of $X(\varepsilon)$.

Theory for mean dilation is simple [13,15]. Coefficients of thermal variation of natural wave speeds c/L in aluminum depend on the coefficients of variation of the elastic moduli, and to a lesser extent the coefficient of thermal expansion [16]. $\delta_S = d \ln(c_{\text{shear}}/L)$ is $-2.9 \times 10^{-4}/^\circ\text{C}$ in aluminum alloys [17]. Similar measurements of the dilatational wave temporal dilation coefficient δ_P are generally less reproducible, so we measured the dilatational wave velocity shift in our materials (using conventional plane wave propagation of 10 MHz plane waves) and determined $\delta_P = d \ln(c_{\text{dilatational}}/L) = -1.685 \pm 0.015 \times 10^{-4}/^\circ\text{C}$. There is some evidence that δ_P varies with plastic strain and alloy, so its precise value is uncertain.

A diffuse wave field is a mix of dilatational and shear waves. In the limit $L \gg \lambda$ we neglect the relatively small contribution of other waves (e.g., Rayleigh surface waves) and consider the field to have a fraction $R/1 + R$ of shear waves and a fraction $1/1 + R$ of longitudinal waves. Here R is the familiar equipartition ratio [18] $R = 2(c_d/c_s)^3$, equal to 16 in aluminum. Thus we predict a mean diffuse field temporal dilation of $\langle \delta \rangle = (R\delta_S + \delta_P)/(R + 1) =$

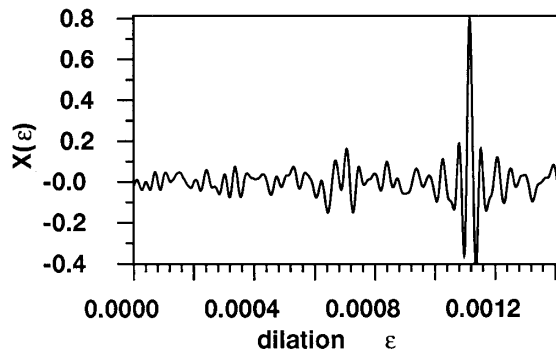


FIG. 3. Normalized cross correlation function $X(\varepsilon)$ for the “big block” taken from 2 msec windows on wide-band signals at age 40 msec and temperatures of 33 and 37 $^\circ\text{C}$. Mean dilation is 1.116×10^{-3} .

$-2.83 \times 10^{-4}/^\circ\text{C}$, largely independent of uncertainties in δ_P , and consistent with the dilation apparent in Fig. 3. Observed dilations varied among our samples, from 2.77 in the big, medium, and small blocks that were cut from the same parent block, to 2.88 in the cylinder and prism (blocks are pictured below).

Theory for distortion is more complicated and is based on a model of the signal as composed of a large number of independent rays, each with its own temporal dilation, each with its own multiply reflected path from source to detector, and each with a history of mode converting reflections from dilatational to shear and back to dilatational. Again we neglect the small number of sojourns as Rayleigh or other waves. In the same spirit of neglecting surface effects compared to those of the bulk, we also neglect variations in ray amplitude due to temperature-dependent changes in reflection coefficients. The change in a ray is thus solely due to the temporal dilations of its dilatational and shear parts. A ray at age A which has spent a time t_P as a dilatational ray and a time $t_S = A - t_P$ as a shear wave will have a net dilation of

$$\delta = [\delta_P t_P + \delta_S t_S]/A = (t_P/A)(\delta_P - \delta_S) + \delta_S.$$

Its mean dilation is given in terms of the mean time spent as a P wave: $\langle t_P \rangle = A/1 + R$, so

$$\langle \delta \rangle = [\delta_P + \delta_S R]/(1 + R).$$

The variance of the ray dilations, at age A , is

$$\text{var} \delta = (\delta_P - \delta_S)^2 \text{var} t_P / A^2.$$

It is a straightforward matter to show that distortion of a narrow band signal composed of rays with a distribution of dilations and no temperature dependence of ray amplitudes, at frequency ω , at age A , and after a temperature shift dT , is given by

$$D = (dT\omega A)^2 \text{var} \delta / 2.$$

The variance $\text{var} t_P$ in the time t_P spent as a longitudinal wave is expected to increase linearly with age A . The rays are taken to randomly mode convert from P to S (and S to P) at rate β (and $\alpha = \beta/R$), such that the mean free time as a longitudinal (shear) wave is $1/\beta$ ($1/\alpha$). The rate of mode conversion is assumed to be independent of the past history of the ray. (This assumption is possibly erroneous; there may be rays with exceptionally long lifetimes in subsets of phase space, especially in objects whose ray trajectories are not chaotic, or which have small Lyapunov exponents.) Another calculation establishes that $\text{var} t_P$ is then given by (at large $A\alpha$ such that many mode conversions have taken place)

$$\begin{aligned} \text{var} t_P &= A^2 \beta \alpha / (\alpha + \beta)^3 \\ &= (2A/\beta) [R^2 / (1 + R)^3] \\ &= 0.104A/\beta. \end{aligned}$$

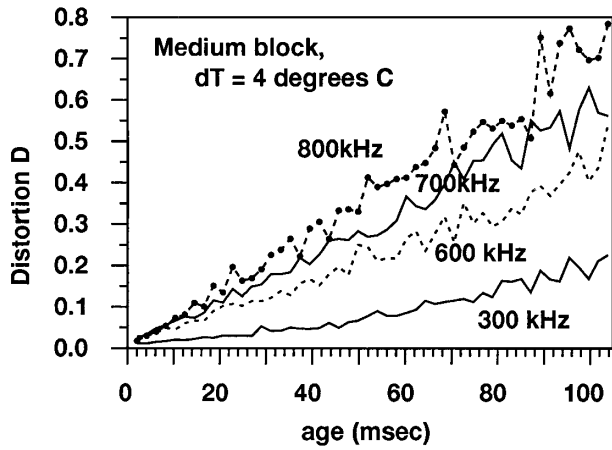


FIG. 4. Distortion rises linearly with age and quadratically with central frequency.

Isotropically distributed diffuse dilatational wave energy of density E_d/V in a volume V is delivered to a bounding surface S at a rate familiar from room acoustics [19] of $c_d S E_d / 4V$. A detailed calculation using the elastic wave reflection coefficients [20] pertaining to aluminum shows that only 59% of this mode converted. Thus we estimate $\beta = 0.59 c_d S / 4 V$.

The above series of assumptions and calculations concludes with a predicted distortion

$$D = 0.356 \omega^2 (\delta_p - \delta_s)^2 dT^2 (A/c_d) (V/S) \\ = C dT^2 f^2 A V/S,$$

which scales quadratically with temperature difference and frequency, and linearly with age and the volume to surface ratio of the sample. On taking the δ 's to be -1.685 and -2.9×10^{-4} , respectively, and c_d to be 6370 m/sec, the coefficient C of that scaling is predicted to be $3.26 \times 10^{-4} / \text{deg}^2 \text{ MHz}^2 \text{ msec cm}$.

The independent ray picture used for the above arguments is inadmissible at times comparable to or greater than the Heisenberg time (density of states) $t_H \approx V \omega^2 / \pi [2/c_s^3 + 1/c_d^3]$ [18] at which the normal modes become distinct. At ages $A > t_H$, responses are better expressed as modal expansions in terms of uncorrelated modes. Taking the fractional change in a natural frequency to be a random number from a distribution with the specified mean $\langle \delta \rangle$, and a variance for which we have at present no theory [21]. It is not difficult to show that distortion in this regime should be quadratic in age and temperature and frequency, with a coefficient which depends on that variance.

Figure 4 shows the measured distortion D for a band with central frequency $f = 300$ kHz and a temperature difference of 4° . The object is the "medium block," illustrated in Fig. 5. The dependence is linear for small ages but steepens noticeably at greater ages. As the Heisenberg time for this object at this frequency is 88 msec, such a steepening is expected. Figure 4 also

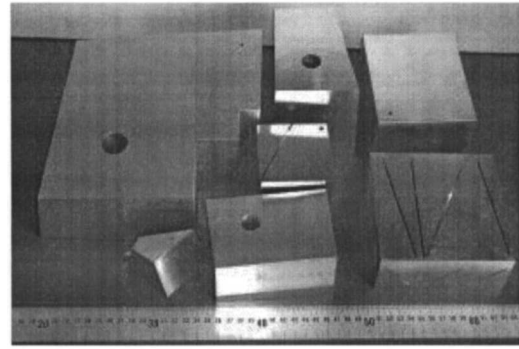


FIG. 5. The aluminum block specimens. Clockwise from the lower left they are the prism ($V = 60.4 \text{ cm}^3$), the big block (2855 cm^3), the medium block (906 cm^3 after extra cut), the rectangle, the cut rectangle (804) pierced by many large scalloped slits, the small block (561), and the cube with one flat-bottomed slit (340). The 10 cm tall \times 18 cm diameter cylinder is not pictured.

shows the expected purely linear age dependence in this block at higher frequencies where the Heisenberg time is greater. The quadratic dependence on frequency is apparent. Figure 6 illustrates the predicted quadratic dependence on temperature difference dT .

As the observed distortions scale well with age, with frequency² and with temperature², it is convenient to summarize all measurements by plotting their apparent coefficients C . Figure 7 compares the theoretical value 3.26×10^{-4} per deg^2 , per MHz^2 , per msec, per cm with that seen in a set of samples, with volumes ranging from 60 to 3000 cm^3 , and volume to surface ratios ranging from 0.6 to 2.5 cm . In all cases dimensionless specimen sizes $L\omega/c_s$ are much greater than unity. Most distortion coefficients lie close to the theoretical prediction. The smallest distortions, those of the prism, the cut rectangle, the small block, and the large block, are those of the samples which one supposes would have ray trajectories which mix rapidly and explore phase space the most quickly and most closely accord with the assumptions of the theory. Their distortions are close to predictions. The greatest distortions, those of the cube with slit,

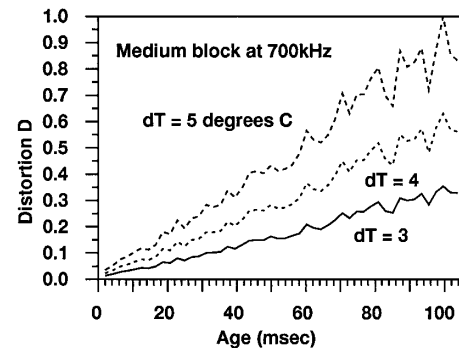


FIG. 6. Distortion is proportional to the square of temperature difference.

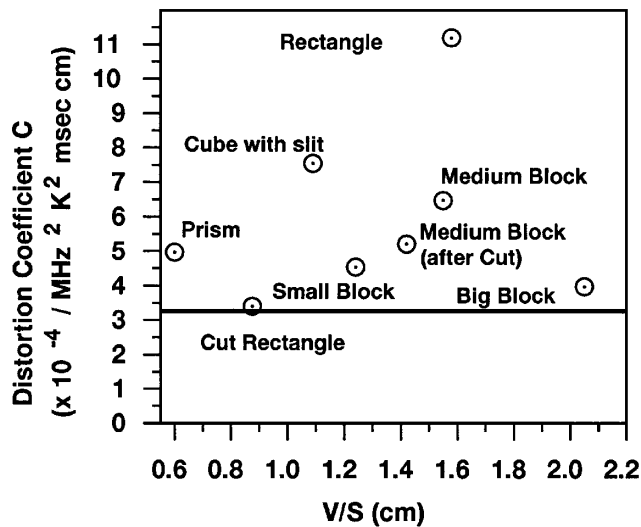


FIG. 7. Observed distortion coefficients C . All values are based on distortions observed at 600 to 900 kHz (except for the prism for which the frequencies were 1200 to 1700 kHz), and 1° to 4° of temperature difference. The case of the cylinder ($C = 38.3$, $V/S = 2.5$ cm) is off the scale. Theory is indicated by the solid line.

the medium block, and most especially the rectangle and the cylinder, are the objects which one considers less chaotic. The cube with a slit is technically only pseudointegrable. The medium block is not, owing to the defocusing surface presented by its hole. One nevertheless argues that the medium block only slowly mixes its ray trajectories. Owing to its near parallel top and bottom surfaces (oblique by 5°) it has “bouncing ball” orbits of exceptionally long life. After an additional more oblique cut which increased this angle to 15° , distortion was lowered by about 20% and brought closer to theory. The cylinder is the most extreme example. Its ray trajectories are integrable and the object has a continuous symmetry. Its distortion is several times greater than any of the others. The theory appears to provide a lower bound on all the observations. This is in accord with the theory’s assumption of a well mixed phase space being a limiting case.

Similar measurements were conducted in aluminum plates. The shorter Heisenberg time there and the plate’s highly dispersive multibranch guided Lamb waves lead to rich behaviors. Distortion is a complex function of frequency. A quantitative theory for distortion in a plate remains unformulated.

Theory for three-dimensional blocks appears to be essentially correct; distortions depend as predicted on age, temperature, frequency, and object geometry. Distortion magnitude is correctly predicted, within about 25%, for the more irregular objects. Distortion magnitude appears to correlate also with the degree of object

irregularity, as if the mixing rate among the modes is least in the more regular objects, thus leading to greater distortion. One can “hear the shape of” these blocks. The dependence on object irregularity suggests that the technique may be useful as a quantum chaos [7] probe of phase space mixing rates, scars, and islands of stability.

This work was supported by NSF Grant No. CMS 99-88645.

- [1] R. L. Weaver, in *Waves and Imaging through Complex Media*, edited by P. Sebbah (Kluwer, Dordrecht, 2001), p. 141.
- [2] A. Derode *et al.*, *J. Acoust. Soc. Am.* **107**, 2987 (2000); C. Draeger and M. Fink, *Phys. Rev. Lett.* **79**, 407 (1997).
- [3] C. Ellegaard *et al.*, *Phys. Rev. Lett.* **77**, 4918 (1996).
- [4] M. L. Cowan *et al.*, *Phys. Rev. E* **65**, 066605 (2002).
- [5] A. Z. Genack and A. A. Chabanov, in *Waves and Imaging through Complex Media* (Ref. [1]), p. 53.
- [6] P. Prabhakar and S. Sridhar, *Phys. Rev. Lett.* **85**, 2360 (2000); A. Kudrolli *et al.*, *Phys. Rev. Lett.* **75**, 822 (1995).
- [7] H.-J. Stöckmann, *Quantum Chaos: An Introduction* (Cambridge University Press, Cambridge, 1999); T. Guhr, A. Müller-Groeling, and H. A. Weidenmüller, *Phys. Rep.* **299**, 189 (1998).
- [8] R. L. Weaver and O. I. Lobkis, *Phys. Rev. Lett.* **84**, 4942 (2000); J. de Rosny *et al.*, *Phys. Rev. Lett.* **84**, 1693 (2000); G. Bayer and T. Niederdrank, *Phys. Rev. Lett.* **70**, 3884 (1993).
- [9] R. L. Weaver, *Wave Motion* **12**, 129 (1990).
- [10] R. Weaver, *J. Acoust. Soc. Am.* **85**, 1005 (1989); C. Ellegaard *et al.*, *Phys. Rev. Lett.* **77**, 4918 (1996).
- [11] R. L. Weaver and O. I. Lobkis, *J. Acoust. Soc. Am.* **110**, 3011 (2001); *Phys. Rev. Lett.* **87**, 134301 (2001); C. Draeger and M. Fink, *J. Acoust. Soc. Am.* **105**, 611 (1996).
- [12] G. Poupinet *et al.*, *J. Geophys. Res.* **89**, 5719 (1984); P. Roberts *et al.*, *J. Acoust. Soc. Am.* **91**, 3291 (1992).
- [13] R. L. Weaver and O. I. Lobkis, *Ultrasonics* **38**, 491 (2000).
- [14] A. Tourin *et al.*, *Phys. Rev. Lett.* **87**, 274301 (2001); S. Yon *et al.*, *J. Acoust. Soc. Am.* (to be published).
- [15] R. Snieder *et al.*, *Science* **295**, 2253 (2002); R. Snieder, *Phys. Rev. E* **66**, 046615 (2002).
- [16] H. Deresiewicz, *J. Acoust. Soc. Am.* **29**, 204 (1957); D. K. Banerjee and Y.-H. Pao, *J. Acoust. Soc. Am.* **56**, 1444 (1974).
- [17] K. Salama and C. K. Ling, *J. Appl. Phys.* **51**, 1505 (1980); E. Chern and J. Heyman, in *Proceedings of the IEEE Ultrasonics Symposium* (IEEE, New York, 1981).
- [18] R. L. Weaver, *J. Acoust. Soc. Am.* **71**, 1608 (1982); R. Hennino *et al.*, *Phys. Rev. Lett.* **86**, 3447 (2001).
- [19] A. D. Pierce, in *Acoustics: An Introduction* (McGraw-Hill, New York, 1981).
- [20] K. F. Graff, in *Wave Motion in Elastic Solids* (Dover, New York, 1991), Sec. 6.1.
- [21] P. Bertelsen *et al.*, *Phys. Rev. Lett.* **83**, 2171 (1999).